

# Synthesis and catalytic behavior of tetrakis(4-carboxyphenyl)porphyrin-periodic mesoporous organosilica

Eun-Young Jeong, Abhishek Burri, Seung-Yeop Lee and Sang-Eon Park\*

Received 9th August 2010, Accepted 8th September 2010

DOI: 10.1039/c0jm02591g

The periodic mesoporous organosilica having the tetrakis(4-carboxyphenyl)porphyrin (TCPP) unit was successfully synthesized by the direct co-condensation method using microwave with the corresponding tetra-silane. The tetra-silane precursor, TCPP-silsesquioxane was prepared through the reaction of TCPP with the APTES(3-Aminopropyltriethoxysilane). And TCPP-PMOs were synthesized with sodium metasilicate as a silica source and P123 (EO20PO70EO20) as a supramolecular template at 100 °C. The TCPP-PMO-*n* (*n* = 2.5 and 5.0, *n* refers to the molar percentage of TCPP precursor per silica) materials had >400 m<sup>2</sup> g<sup>-1</sup> of specific surface areas with ~8.7 nm of pore diameter. TCPP-PMOs were illustrated to give superiority in the organocatalytic hydrogen transfer reactions of various ketones such as acetophenone, cyclohexanone and pinacolone as well as good activity in the photocatalytic degradation of methylene blue (MB) without metal incorporation. Fe-TCPP-PMO prepared by ion-exchange method gave also good activity and selectivity in the oxidation of cyclohexene.

## 1. Introduction

Organic–inorganic hybrid materials with periodic mesoporosity have attracted much attention in recent years, owing to their symbiotic properties, which make it quite possible to use them in applications such as separation, photonics, nanoelectronics, drug delivery, and heterogeneous catalysis.<sup>1–4</sup> Mesoporous organic–inorganic hybrid materials can be synthesized by incorporating organo functionalities using three different methods. The first is called grafting or the post synthetic method, which is formed by the subsequent anchoring of organic silanes onto a silica matrix. The other co-condensation method involves the self-assembly of inorganic silica precursors and organosilanes in one-pot. And the third is the unique attachment of organic functions to the siliceous wall by using organic bridged alkoxy silane precursors entirely or partially with silica source, which are named as periodic mesoporous organosilicas (PMOs).

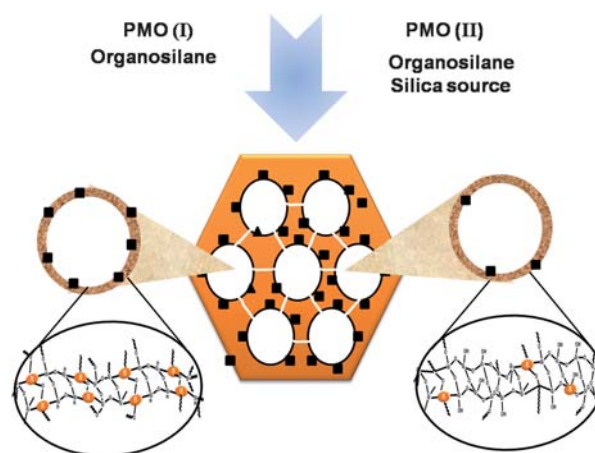
Periodic mesoporous organosilicas (PMOs) are a special type of ordered mesoporous silica in which organic moieties are integrated onto the silica framework entirely or randomly to form hybrid organic–inorganic materials. The most important feature of PMOs are that they can incorporate various organo functionalities into inorganic frameworks to form organic–inorganic hybrid materials of which diverse organo-functionalities offer broad application.

The organic moieties of PMOs mainly rely on various silsesquioxanes of such as disilanes, trisilanes, and tetrasilanes with different organic bridging groups. Their syntheses were started at the end of the twentieth century with three independent groups. Soon after, many trials were conducted for the integration of organic moieties into silica frameworks.<sup>5–10</sup> They can be classified into two types of PMOs. Generally, PMO-I is composed entirely of organo groups on the walls with regular form. This is prepared

totally by using bridged organosilanes alone.<sup>10–13</sup> Some of PMOs have random or partial organo groups on the wall, which are usually synthesized using both bridged organo silanes together with silica sources (PMO-II) (Scheme 1).<sup>14</sup>

As the bridging organic moieties, short aliphatic chain-like methane, ethane, and ethylene, aromatic groups of phenylene,<sup>7</sup> biphenylene, and xylene have been used mostly in the form of disilanes. However, organosilane precursors in the form of trisilanes and tetrasilanes were rarely used.<sup>15,16</sup>

An ethane-isocyanurate bridged PMO was synthesized simply by using tris[3-(trimethoxysilyl)propyl]isocyanurate and 1,2-bis(triethoxysilyl)ethane in the presence of a triblock copolymer by Jaroniec and his coworkers.<sup>11</sup> Park *et al.* prepared melamine-bridged PMOs with high reproducibility by co-condensation using N<sup>2</sup>,N<sup>4</sup>,N<sup>6</sup>-tris(3-(triethoxysilyl) propyl)-1,3,5-triazine-2,4,6-triamine (TBTS) and sodium metasilicate in the presence of P123 (P123, EO20PO70EO20) at a highly acidic concentration.<sup>17</sup> Corriu *et al.* prepared PMOs with tetraazacyclotetradecane



Scheme 1 Two types of PMO-I and PMO-II.

Laboratory of Nano-Green Catalysis and Nano Center for Fine Chemical Fusion Technology, Department of Chemistry, Inha University, Incheon, 402-751, Korea. E-mail: separk@inha.ac.kr; Fax: +82 32 872 8670

moieties using TEOS in the presence of Pluronic 123(P123) and NaF with high yield, and a narrow pore size distribution.<sup>15</sup> Recently, Ozin *et al.* synthesized C<sub>60</sub>-PMO by assembling C<sub>60</sub> and TEOS with P123.<sup>14</sup>

Porphyrin has been utilized in various applications, for example, catalysis, photosynthesis, photodynamic therapy,<sup>18</sup> and sensors.<sup>19</sup> But it has a planar structure with a macrocycle of four pyrrole rings connected by methine bridges. Consequently, it is difficult to assemble porphyrin-tetrasilane owing to its entirely flat structure. To resolve this issue, we tried to synthesize type II PMO by using porphyrin-tetrasilane with sodium metasilicate as a silica source. The use of this silica source is expected to lower the concentration of the organic group in the periodic mesoporous silica. But the silica source promote the self-assembly of organosilanes.

However, there are no reports on porphyrin in PMO materials up to now. Herein, we report on PMOs containing tetrakis(carboxyphenyl)porphyrin (TCPP). TCPP-PMO(II) is notable as the first report in the field of periodic mesoporous organosilica.

Also, microwave digestion was adopted for the synthesis of PMOs in order to facilitate the assembly of organosilane. Smeulders *et al.* synthesized a benzene-PMO under microwave irradiation.<sup>20</sup> Benzene bridged PMOs is prepared by use of microwave heating which can achieve a reduction in a synthesis time of several hours up to several days. In addition, the benzene bridged PMOs synthesized by microwave irradiation exhibit better porosity characteristics while maintaining their molecular and mesoporous ordering.<sup>20</sup> Besides those, generally microwave synthesis offers several advantages such as rapid and homogeneous heating of the entire sample, improved reaction rates, ease in formation of uniform nucleation centers<sup>21</sup> and rapid crystallization, and environment friendly due to energy saving.<sup>22</sup> Microwave synthesis also simplifies the process for obtaining, well-ordered mesoporous structures with enhanced hydrothermal stability.

Here, we report the synthesis of periodic mesoporous organosilicas with TCPP-silsesquioxane as a tetra silane. All the catalysts described herein were synthesized by the direct co-condensation method using microwaves as a heating source. The TCPP-tetrasilane linked in periodic mesoporous organosilica, denoted as TCPP-PMO(II), was synthesized by self-assembly of TCPP-tetrasilane (prepared in our laboratory) together with sodium metasilicate as a surplus silica source and poly(ethylene

oxide)-poly(propylene oxide)-poly(ethylene oxide) triblock copolymer under acidic conditions (Scheme 2). And the synthesized TCPP-PMO(II) were applied to the hydrogen transfer reaction, cyclohexene oxidation and methylene blue degradation under visible light were investigated.

## 2. Experimental

### 2.1. Materials

The surfactant Pluronic P123 (EO<sub>20</sub>PO<sub>70</sub>EO<sub>20</sub>; MW5800 BASF) was used as the template. Sodium metasilicate (Na<sub>2</sub>SiO<sub>3</sub>·9H<sub>2</sub>O; Sigma Aldrich) was used as silica source. Amino propyl triethoxy silane (Aldrich) was used for preparing tetra-silane with tetrakis(4-carboxyphenyl)porphyrin. Hydrochloric acid was purchased from Daejung Chemical Company, Korea. Other chemicals used for catalytic application were purchased either from Aldrich or TCI Tokyo Kasei with high purity. All the chemicals were used as received without any further purification.

### 2.2. Synthesis of tetrakis(4-carboxyphenyl)porphyrin(TCPP)

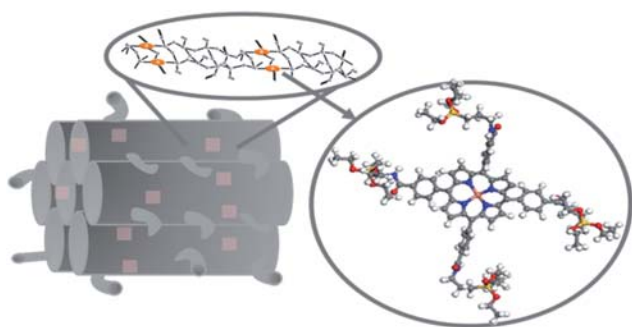
Pyrrole (2.33 mmol) and 4-carboxybenzaldehyde (2.33 mmol) were dissolved in 100 ml propionic acid and stirred for 4 h at 120 °C. Then the product solution was cooled to room temperature, and methanol was added and continued to be chilled in an ice bath with stirring. The deep-purple crystals were precipitated, filtered and washed using methanol and hot water. The resulting solid was dissolved in chloroform containing 2% acetone and purified by column chromatography over silica gel using chloroform as an eluent.

### 2.3. Synthesis of TCPP-silsesquioxane

In a round bottom flask, 3-aminopropyltriethoxysilane (4 mmol) and dicyclohexyl carbodiimide (4 mmol) were suspended in 50 ml of tetrahydrofuran (THF). The TCPP (1 mmol) was dissolved in 5 ml of THF and added drop-wisely. The flask was evacuated and flushed with nitrogen gas. The mixture was refluxed overnight under nitrogen atmosphere. After cooling down to room temperature, the product was washed with petroleum ether.

### 2.4. Preparation of TCPP-silsesquioxane bridged mesoporous organosilica

TCPP-bridged PMOs were prepared by TCPP- silsesquioxane and sodium metasilicate with Pluronic P123 (EO<sub>20</sub>PO<sub>70</sub>EO<sub>20</sub>, Aldrich) and c-HCl. In a typical synthesis, 166 ml of triblock copolymer P123 in deionized water (DW) and 126 ml of sodium metasilicate solution was mixed to form a clear solution with stirring. Then organosilane precursor and hydrochloric acid (37.6%) was quickly added to the clear solution. The mixture was aged at 40 °C for 1 h with stirring and heated at 100 °C for 2 h under microwave irradiation (300 W, 100%, CEM Mars 5). The solid product was filtered and washed with copious amount of water and ethanol. And further removal of the surfactant was performed by soxhlet extraction using ethanol and hydrochloric acid (*v* : *v* = 97 : 3) for 4 h. The resulted products were represented as TCPP-PMO-*n* (*n* refers to the molar percentage of TCPP-Silsesquioxane). The composition of final mixture was



**Scheme 2** The illustration of Tetrakis(4-CarboxyPhenyl)Porphyrin (TCPP)-Silsesquioxane bridged PMO.

$(1-x)\text{SiO}_2 : x\text{TCPP-tetrasilane} : 0.018\text{P123} : 1\text{HCl} : 117.1\text{H}_2\text{O}$   
 $(x = \text{TCPP-tetrasilane}/(\text{TCPP-tetrasilane} + \text{SiO}_2)) = 0.025$  and 0.05).

### 2.5. Preparation of Fe-TCPP-silsesquioxane bridged mesoporous organosilica

TCPP-PMO-5 (1.0 g) was suspended in 25 ml of DMF in a bottom round flask followed by addition of  $\text{FeCl}_2 \cdot 4\text{H}_2\text{O}$  (2.0 mmol). The system was heated at 120 °C during 4 h with mechanical stirring and under nitrogen atmosphere. The crude product was exhaustively washed in a Soxhlet extractor with DMF, methanol and  $\text{CH}_2\text{Cl}_2$ . The Fe-(TCPP)-PMO was washed with deionized water. The solid was washed again in the Soxhlet extractor with methanol and Fe(TCPP)-PMO was dried at 80 °C per 24 h.

### 2.6. The photocatalytic degradation of methylene blue

The photocatalytic degradation of methylene blue was carried out at room temperature. A quartz calorimetric vessel was used as photocatalytic reaction apparatus. The vessel was filled with the MB solution ( $1.16 \times 10^{-5} \text{ mol dm}^{-3}$ ). The TCPP-PMO-2.5 was immersed in the solution. High pressure XE lamp ranging 230–800 nm was used with cutoff filter (UV-390) as a visible lay. The photodegradation of methylene blue was monitored by observing -660 nm of the characteristic peaks of methylene blue using UV-visible spectroscopy. The reference was aqueous solution of methylene blue with no TCPP-PMO.

### 2.7. Hydrogen transfer reaction

Hydrogen transfer reaction of ketones such as acetophenone, cyclohexanone and pinacolone were conducted in liquid phase reaction. 20 mg catalyst (preactivated at 393 k prior to use) was added to 3.0 mL 2-propanol. To this mixture, 0.19 mmol of KOH and 1 mmol ketones was added and reacted at 80 °C during 5 h. The aliquots of the reaction mixture were withdrawn and subjected to GC analysis (Agilent 6890N, DB-WAX capillary column, FID detector).

### 2.8. Catalytic oxidation of cyclohexene

The oxidation of cyclohexene was performed in a conventional glass reactor (50 ml) with a condenser and stirrer of which reactor was loaded with 0.05 g catalyst, cyclohexene (5 mmol), 10 ml acetonitrile and 10 mmol of 30% aqueous  $\text{H}_2\text{O}_2$ . The catalyst was activated at 250 °C for 4 h before loading into the glass reactor. The reaction was monitored by analyzing the reaction samples at different time intervals by a gas chromatograph (HP-6890) equipped with a HP-5 capillary column and a FID detector and oven temperature were programed from 70 °C to 200 °C with a heating rate of 10 °C  $\text{min}^{-1}$ . Conversion of cyclohexene and products selectivity was calculated based on the GC analysis.

### 2.9. Characterization of TCPP-PMO-*n*

The XRD patterns were obtained by using a Rigaku Multiflex diffractometer with a monochromated high-intensity Cu-K $\alpha$  radiation ( $\lambda = 1.54 \text{ \AA}$ ). Scanning was performed under ambient

conditions over the  $2\theta$  region of 0.7–5° at the rate of 0.1°  $\text{min}^{-1}$  (20 kV, 10 mA). Elemental ratio (C/N) was measured using EA1112. The scanning electron microscope (SEM) images were observed using a JEOL 630-F microscope. Before the measurement, the samples were dispersed onto a steel plate surface and coated with Pt metal. Transmission electron microscope (TEM) images were observed using a JEM-3011 instrument (JEOL) equipped with a slow-scan CCD camera operating at 300 keV. Solid-state NMR spectra were collected through a DSX Bruker NMR 600 MHz. The  $\text{N}_2$  adsorption-desorption isotherms and pore characterization were obtained by using a Micromeritics ASAP 2020 apparatus at liquid  $\text{N}_2$  temperature. Thermogravimetric analysis (Bruker 2010 SA) were carried out to detect the decomposition temperature of the organic moieties grafted on the mesoporous silica. The tetrakis(4-carboxyphenyl)porphyrin was analyzed by UV-Vis-NIR spectroscopy (SolidSpec-3700).

## 3. Results and discussion

### 3.1. Characterization of TCPP-PMO

The low-angle powder X-ray diffraction patterns of TCPP-PMO-2.5 and TCPP-PMO-5 are shown in Fig. 1(a). All the samples showed three well-resolved diffraction peaks with a very intense peak at  $2\theta = 0.9$ –1.18 and two peaks at  $2\theta = 1.4$ –1.8. These peaks could be indexed to the (100), (110), and (200) planes respectively, which correspond to a mesostructure of hexagonal space group symmetry  $p6mm$ . The strong (100) peak was maintained well in both TCPP-PMO (II). All the  $\text{N}_2$  adsorption and desorption isotherms of the samples were type IV, with type H1 hysteresis loops at high relative pressures (Fig. 1b). The surface area, pore diameter and elemental analysis for TCPP-PMO-*n* are shown in Table 1. The surface area is evaluated from nitrogen adsorption isotherms by using the BET equation. Pore size was calculated by the Barrett-Joyner-Halenda (BJH) method using the desorption branch of the adsorption-desorption isotherms. When the TCPP tetra silane content increases from 2.5% to 5%, the pore diameters curves shift from 8.7 nm to 8.5 nm. The wall thickness increases from 3.6 nm to 3.7 nm. The tendency of mesopore shrinkage with increasing TCPP tetra silane loading is also exhibited by changes in the surface area and total pore volume, which indicate worse mesostructural features

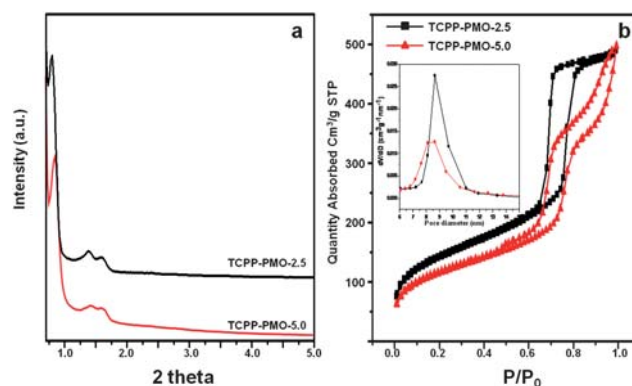


**Fig. 1** (a) Powder XRD patterns of samples TCPP-PMO-2.5 and TCPP-PMO-5 and (b)  $\text{N}_2$  adsorption-desorption and pore size distribution (inset) of samples TCPP-PMO-2.5 and TCPP-PMO-5.

**Table 1** Structural, textural and compositional information of TCPP-PMO-*n*

Sample	$d_{100}/\text{nm}$	BET surface area/ $\text{m}^2 \text{g}^{-1}$	Pore diameter/ $\text{nm}^a$	Total pore volume/ $\text{cm}^3 \text{g}^{-1}$	$a_0/\text{nm}^b$	Wall thickness/ $\text{nm}^c$	Elemental analysis C/N ratio
TCPP-PMO-2.5	10.6	493	8.7	0.78	12.4	3.6	6.43
TCPP-PMO-5.0	10.3	403	8.5	0.76	12.1	3.7	6.67

<sup>a</sup> Pore diameter was calculated from desorption branch by BJH method. <sup>b</sup>  $a_0 = 2d_{100}/\text{root } 3$ . <sup>c</sup> Wall thickness =  $a_0$ -pore size.

with higher loading of TCPP groups. In elemental analysis data, the expected C/N ratio of TCPP-tetrasilane was 6.51 and the ratio observed were 6.43(TCPP-PMO-2.5) and 6.67(TCPP-PMO-5.0) which states that maximum amount of organosilane was introduced into the PMO.

Fig. 2 shows (a, b) transmission electron microscopy (TEM) images and (c, d) scanning electron microscopy (SEM) images of the obtained TCPP-PMOs. The SEM images reveal shorter channel lengths and hexagonal shape morphology. The TEM images indicate that the lengths of the mesopore channels were in the submicromet range and that the channel directions of the 2D-hexagonal structures were parallel to the vertical direction of the hexagonal platelet morphology. TCPP-PMO-*n* would be explained to have a hexagonal space group symmetry  $p6mm$  of high orderliness in good agreement with XRD data.

TCPP unit bridged into mesoporous silica was checked by UV-DR spectroscopy and photoluminescence spectroscopy (Fig. 3). From the UV-DR spectra, the TCPP had the Soret band at 417 nm and four Q-bands at 513, 548, 591 and 649.<sup>23</sup> The TCPP unit in the bridged mesoporous organosilica had absorption bands at 413 (Soret band) and four Q-bands at 514, 548 and 591, 647 nm. Compared with the TCPP compounds, the Soret band of the TCPP-PMO was shifted toward shorter wavelengths. This could be explained due to the interactions of the porphyrin with periodic mesoporous organosilica. When the TCPP was functionalized into the mesoporous silica walls, interactions of the ligand of the TCPP with their chemical environment changed

the symmetry of the porphyrin. It was appeared as the shifts of the absorption bands toward higher energy.

The emission spectra of TCPP-PMO-*n* with different loading levels are presented in Fig. 3. TCPP-PMO-2.5 shows these two wavelengths at 646 nm and 705 nm. The emission peak at 646 nm coincides with the longest wavelength peak in the absorption spectrum and thus could be assigned as the (0,0) component of  $Q_x$ . TCPP-PMO-5 exhibits two peaks at 650 nm and 706 nm. For TCPP-PMO-*n*, the emission spectra exhibit a red shift from 646 nm to 650 nm and peak broadening was observed with increasing of TCPP loadings. The reason is that the increase of the concentration of TCPP-unit could increase the intermolecular interactions between TCPP-unit and silica on the walls. This might cause the formation of excimers between adjacent lumophores in the walls.<sup>24,25</sup>

TCPP bridged mesoporous silica was confirmed by TG-DTA measurements (Fig. 4). The free TCPP decomposed into several steps during heating upto 800 °C. An exothermic loss in weight of 23% appeared at 345 °C and additional weight loss of 70% was followed at 437 °C. The overlap of two steps in the TG curve could be distinguished by the corresponding DTA curve. From the loss in weight, we tentatively assign these steps to the successive cleavage of TCPP unit. TCPP-PMO-*n* shows somewhat different decomposition behaviour due to covalent interactions between TCPP unit and mesoporous silica. The TG-DTA curve of TCPP-PMO shows less defined weight loss steps and peak maxima. A broad exothermic DTA peaks between 300 °C and 600 °C were observed. The TCPP-PMO-2.5 decomposed more rapidly than TCPP-PMO-5 and completed at *ca.* 500 °C. Weight losses at 200–350 °C and 360–480 °C for TCPP-PMO were assigned to loss of carboxyl and phenyl groups from porphyrin, respectively. A second weight loss in the range

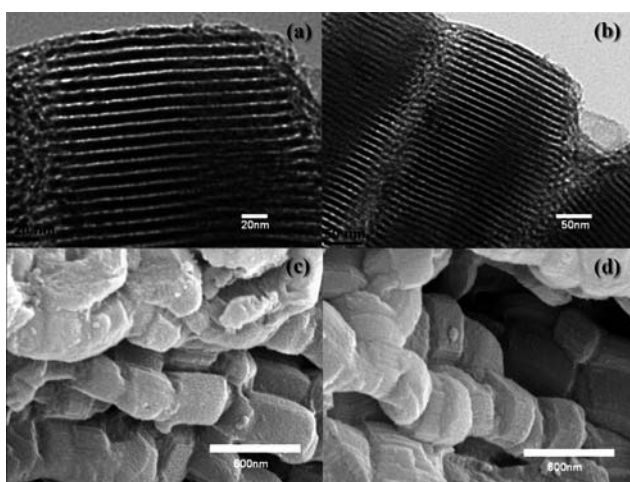


**Fig. 2** TEM (top) and SEM (bottom) images of TCPP-PMO-2.5 (a,c) TCPP-PMO-5 (b,d).

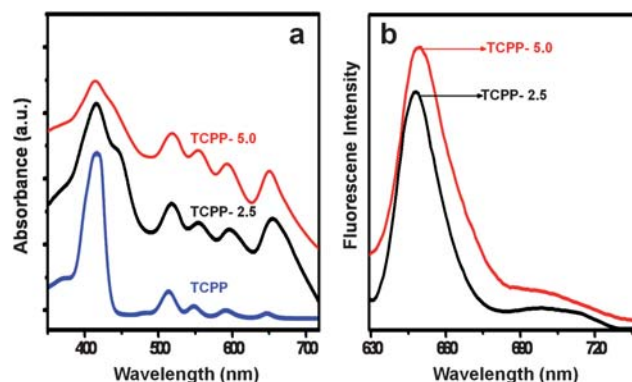


**Fig. 3** UV-Vis spectra (a) and fluorescence spectra (b) of TCPP-PMO-2.5 and TCPP-PMO-5.

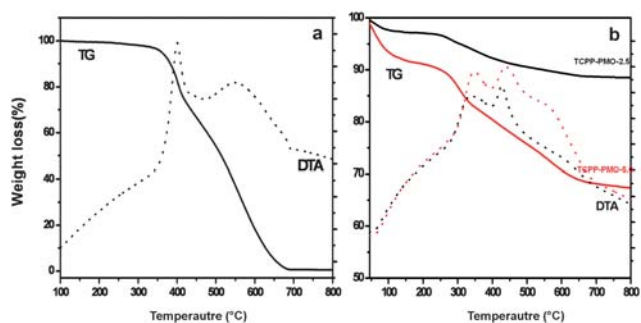


Fig. 4 TG-DTA curves of (a) free TCPP and (b) TCPP-PMO- $n$  ( $n = 2.5$  and 5).

500–627 °C was attributed to the decomposition of the porphyrin rings. The weight losses of the bridged TCPP unit in TCPP-PMO-2.5 and TCPP-PMO-5 were 0.1 mmol g<sup>-1</sup> and 0.29 mmol g<sup>-1</sup>, respectively.

In order to obtain information about the chemical environment of silicon atoms presented in the materials, <sup>29</sup>Si CP MAS NMR experiment was done and shown in Fig. 5. Two T<sup>n</sup> and three Q<sup>n</sup> signals, which could be assigned to the following Si species: T<sup>2</sup> [C–Si(OSi)<sub>2</sub>(OH),  $d = -58$  (5.17%)]; T<sup>3</sup> [C–Si(OSi)<sub>3</sub>,  $d = -66.01$  (13.63%)]; Q<sup>2</sup> [Si(OSi)<sub>2</sub>(OH)<sub>2</sub>,  $d = -91.0$  (10.64%)]; Q<sup>3</sup> [Si(OSi)<sub>3</sub>(OH),  $d = -100$  (49.2%)]; Q<sup>4</sup> [Si(OSi)<sub>4</sub>,  $d = -109.8$  (20.93%)]. The spectra of the samples exhibit two signals at around –58 and –67 ppm which could be assigned to T<sup>2</sup> and T<sup>3</sup>

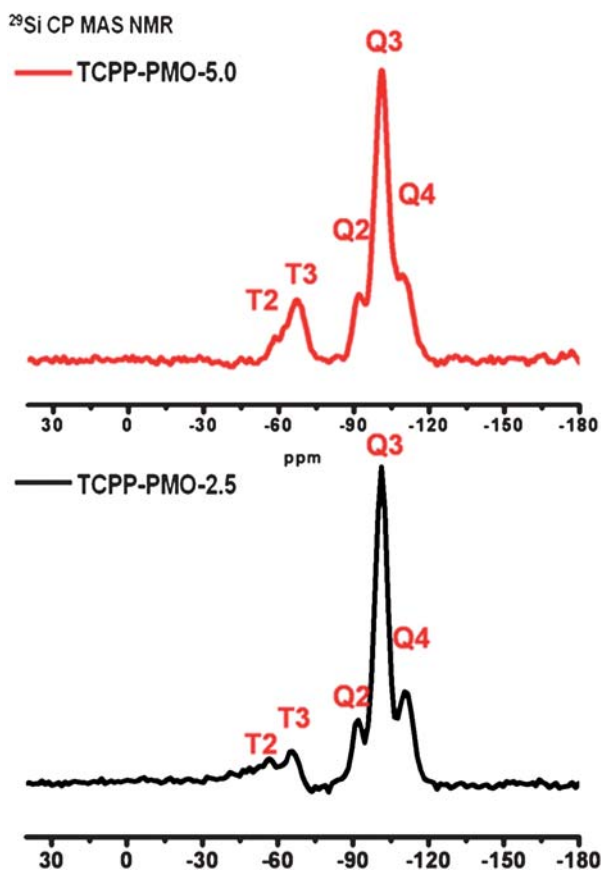


Fig. 5 <sup>29</sup>Si solid state NMR spectra of TCPP-PMO-2.5 and -5.

resonances, respectively. The presence of T<sup>2</sup> and T<sup>3</sup> resonances proved that the functional groups of TCPP units were functionalized in the silica wall. The signals at –91, –100 and –109.8 ppm are due to Q<sup>2</sup>, Q<sup>3</sup> and Q<sup>4</sup> sites, respectively. So, TCPP-PMO, showed the presence of both Q<sup>3</sup> [Si(OSi)<sub>3</sub>(OH)] and Q<sup>4</sup> [Si(OSi)<sub>4</sub>] with T<sup>2</sup> and T<sup>3</sup> sites, which indicates the condensation reaction between the organosilane and silica species.

### 3.2. Catalytic applications of TCPP-PMO

The photocatalytic activities of pure SBA-15, TCPP-PMO-2.5 and no catalyst were evaluated by measuring the decomposition rates of methylene blue under the visible light irradiation (>390 nm). Fig. 6 shows the changes of MB concentrations with reaction time in the presence of TCPP-PMO-2.5 and without catalyst under the visible light. The visible-light without any catalyst gave only about 4% decomposition of MB molecules within 2 h. TCPP-PMO-2.5 sample shows superior photocatalytic activity with 55% degradation rate of MB within 2 h under the same condition (Fig. 6). This could be explained by two reasons. One is that the contribution of TCPP moiety on the surface of silica, resulted in the production of more photoinduced electrons and holes, and another reason is that the formed O=C–NH bond between TCPP and tetra-silane played an important role in the electron transfer channel by accelerating electron injection.<sup>26,27</sup>

Organocatalysis can be performed by organofunctionalized mesoporous materials as green approaches. In this context, TCPP-PMOs were applied to the catalytic hydrogen transfer reaction, which has been important to produce key intermediates for the synthesis of pharmaceuticals and agrochemicals. As ketones, acetophenone and cyclohexanone and pinacolone were chosen with isopropylalcohol as a hydrogen transfer agent. In the case of acetophenone as a reactant, the conversion over TCPP-PMO-2.5 and 5 reached 17% and 30%, respectively. Fig. 7 shows that the increasing rate of conversion over TCPP-PMO-5 was two-times higher than those over TCPP-PMO-2.5. The results could be explained by the morphological advantage and higher loadings of porphyrin as active sites onto TCPP-PMO. It is well accepted that the diffusion and mass transfer of reactant

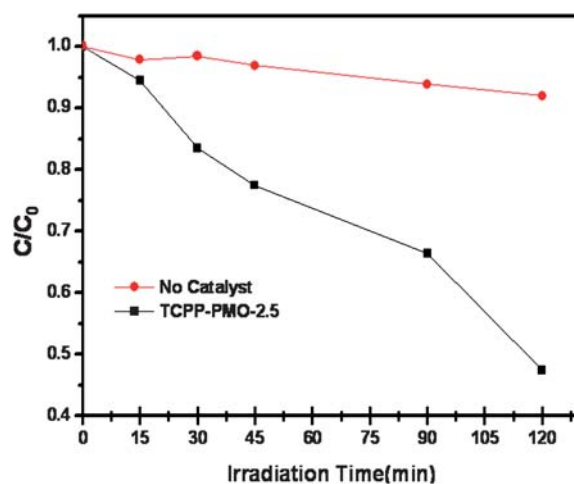


Fig. 6 Photocatalytic degradation of MB, in the presence of TCPP-PMO-2.5 and without catalyst under the visible light.

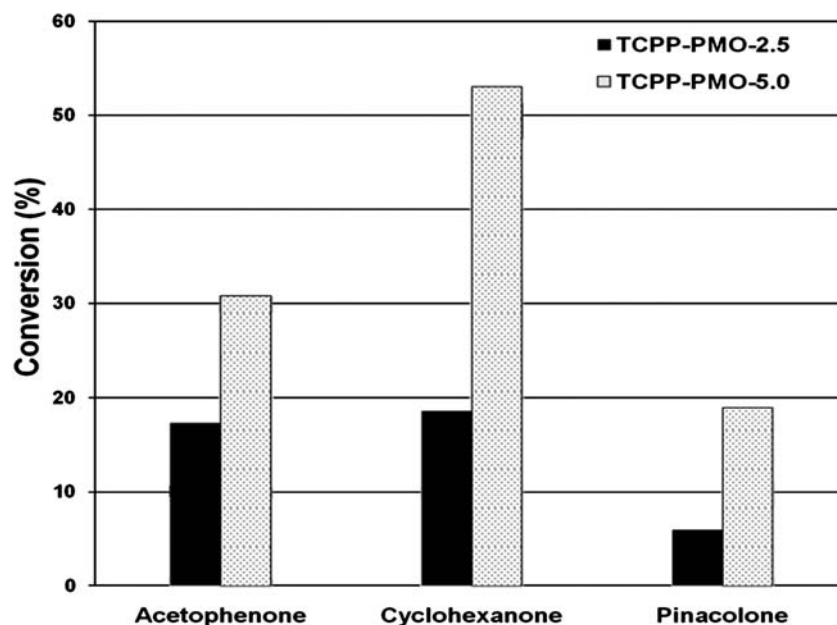


Fig. 7 Transfer hydrogenation of ketones over TCPP-PMO-2.5 and TCPP-PMO-5.

molecules into the pores to reach the active sites have great influence on liquid-phase heterogeneous catalytic reactions.<sup>28</sup> Both TCPP-PMO catalysts gave perfect selectivity toward only one desired alcohol product. In addition to, cyclohexanone over TCPP-PMO-5 gave better conversion (about 60%) than acetophenone was used as a reactant. Also, all TCPP-PMOs gave good catalytic activities for hydrogenation of acetophenone and cyclohexanone with perfect selectivity. Slightly low activity was obtained only in the case of pinacolone. As for leaching test, TCPP-2.5 and TCPP-5 were separated after 5 h reaction and washed. After washing, the same reaction condition was applied repeatedly. The catalysts showed similar activities, which meant no significant loss of the active sites were ascribed to no serious leaching out during reaction process.

Finally, the oxidation of cyclohexene was investigated over Fe-TCPP-PMO-2.5 and the results are shown in Table 2. In the oxidation of cyclohexene using hydrogen peroxide, cyclohexene oxide, 2-cyclohexene-1-one, 2-cyclohexene-1-ol and 1,2-cyclohexanediol were formed. The Fe-TCPP-PMO catalyzed

cyclohexene could promote the oxidation of the double bond to form correspondingly epoxide. It is indicated that conversion of cyclohexene increased with the increase in  $\text{H}_2\text{O}_2/\text{cyclohexene}$  mole ratio (1 to 3). Maximum cyclohexene conversion of 41.5% was obtained in 3 of  $\text{H}_2\text{O}_2/\text{cyclohexene}$  mole ratio at 60 °C. However, the selectivities for cyclohexene epoxide remained the same in all  $\text{H}_2\text{O}_2/\text{cyclohexene}$  mole ratios. The selectivity for 2-cyclohexene-1-ol was found to be maximum (35.8%) with  $\text{H}_2\text{O}_2/\text{cyclohexene}$  mole ratio of 1. But the selectivities on 2-cyclohexene-1-ol were decreased in larger amounts of  $\text{H}_2\text{O}_2$ . Because higher hydrogen peroxide amounts led to further oxidation to give 1, 2-cyclohexanediol during the cyclohexene oxidation. The activities of Fe-TCPP-PMO-2.5 at different temperatures were also tested. The activity results of Fe-TCPP-PMO are given in Table 2. It seems that conversion of cyclohexene was dependent on temperatures. The rates increased with the increase in temperatures. The activation energy was calculated 24  $\text{kJ mol}^{-1}$  from the Arrhenius equation by plotting the graph of  $-\ln(\text{rate})$  vs.  $1/T$ . The oxidation of cyclohexene to

Table 2 Oxidation of cyclohexene with  $\text{H}_2\text{O}_2$  over TCPP-PMO<sup>a</sup>

Entry	$\text{H}_2\text{O}_2/\text{Cyclohexene}$ Ratio	$T/^\circ\text{C}$	Cyclohexene Conv. (%)	Product selectivity (%) <sup>b</sup>			
				Epoxide	Cyclo-one	Cyclo-ol	Cyclo-diol
1	1	60	20.5	19.1	37.0	35.8	8.0
2	2	60	36.5	17.9	35.4	34.0	12.6
3 <sup>d</sup>	3	60	41.5	16.4	34.5	34.4	14.1
4 <sup>c</sup>	3	60	10.5	12.5	34.6	33.0	19.7
5 <sup>d</sup>	3	25	6.5	34.0	29.6	28.5	3.5
6 <sup>d</sup>	3	40	30.1	25.7	33.0	31.2	9.7
7 <sup>e</sup>	3	40	0	—	—	—	—

<sup>a</sup> Reaction conditions: Catalyst = 50 mg, Temp. = 60 °C and Time = 5 h. <sup>b</sup> Legend: Cyclo-oxide = Cyclohexene oxide; Cyclo-one = 2-cyclohexene-1-one; Cyclo-ol = 2-cyclohexene-1-ol; Cyclo-diol = 1, 2-cyclohexanediol. <sup>c</sup> Iron-TCPP complex (homogeneous). <sup>d</sup> Used for calculating of activation energy. <sup>e</sup> Pure SBA-15(blank catalytic test).

provide oxygenates is endothermic in nature (enthalpy,  $\Delta H^\circ = \Delta E_a - RT = 6.5 \text{ kJ mol}^{-1}$ ). As shown in the Table 2, Fe-TCPP-PMO-2.5 gave good activity which was presumably due to high-valent iron–oxo porphyrin as the oxidizing species. And also higher conversions of cyclohexene showed the decreased selectivities on cyclohexene epoxide due to further oxidation which led to the formation of other products.

#### 4. Conclusion

In conclusion, TCPP bridged periodic mesoporous organosilica was successfully synthesized and played a role as an efficient catalyst in photodegradation of MB and especially in the hydrogen transfer reaction by taking advantages of mesoporosity and porphyrin functionality. Also, the Fe-TCPP-PMO exhibited a high catalytic activity in the oxidation of cyclohexene with hydrogen peroxide. The reaction results showed high selectivity to 2-cyclohexen-1-one and 2-cyclohexene-1-ol with conversion up to 41% after a 5 h reaction.

#### Reference

- 1 S. Inagaki, S. Guan, Y. Fukushima, T. Ohsuna and O. Terasaki, *J. Am. Chem. Soc.*, 1999, **121**, 9611–9614.
- 2 B. J. Melde, B. T. Holland, C. F. Blanford and A. Stein, *Chem. Mater.*, 1999, **11**, 3302–3308.
- 3 T. Asefa, M. J. MacLachlan, N. Coombs and G. A. Ozin, *Nature*, 1999, **402**, 867–871.
- 4 B. Hatton, K. Landskron, W. Whitnall, D. Perovic and G. A. Ozin, *Acc. Chem. Res.*, 2005, **38**, 305–312.
- 5 T. Asefa, M. Kruk, M. J. MacLachlan, N. Coombs, H. Grondey, M. Jaroniec and G. A. Ozin, *J. Am. Chem. Soc.*, 2001, **123**, 8520–8530.
- 6 M. C. Burleigh, S. Jayasundera, M. S. Spector, C. W. Thomas, M. A. Markowitz and B. P. Gaber, *Chem. Mater.*, 2004, **16**, 3–5.
- 7 W. J. Hunkeler and G. A. Ozin, *Chem. Mater.*, 2004, **16**, 5465–5472.
- 8 A. Sayari and S. Hamoudi, *Chem. Mater.*, 2001, **13**, 3151–3168.
- 9 J. Morell, G. Wolter and M. Froba, *Chem. Mater.*, 2005, **17**, 804–808.
- 10 M. A. Wahab, H. Hussain and C. He, *Langmuir*, 2009, **25**, 4743–4750.
- 11 R. M. Grudzien, B. E. Grabicka, S. Pikus and M. Jaroniec, *Chem. Mater.*, 2006, **18**, 1722–1725.
- 12 S. Inagaki, S. Guan, T. Ohsuna and O. Terasaki, *Nature*, 2002, **416**, 304–307.
- 13 S. S. Park, D. H. Park and C.-S. Ha, *Chem. Mater.*, 2007, **19**, 2709–2711.
- 14 W. Whitnall, L. Cademartiri and G. A. Ozin, *J. Am. Chem. Soc.*, 2007, **129**, 15644–15649.
- 15 R. J. P. Corriu, A. Mehdi, C. Reye and C. Thieuleux, *Chem. Commun.*, 2002, 1382–1383.
- 16 B. Johnson-White, M. Zeinali, A. P. Malanoski and M. A. Dinderman, *Catal. Commun.*, 2007, **8**, 1052–1056.
- 17 E. A. Prasetyanto, M. B. Ansari, B.-H. Min and S.-E. Park, *Catal. Today*, 2010, DOI: 10.1016/j.cattod.2010.03.081.
- 18 I. Scalise and E. N. Durantini, *J. Photochem. Photobiol., A*, 2004, **162**, 105–113.
- 19 B. Johnson-White, M. Zeinali, K. M. Shaffer, C. H. Patterson Jr., P. T. Charles and M. A. Markowitz, *Biosens. Bioelectron.*, 2007, **22**, 1154–1162.
- 20 G. Smeulders, V. Meynen, G. V. Baelen, M. Mertens, O. I. Lebedev, G. V. Tendeloo, B. U. W. Maes and P. Cool, *J. Mater. Chem.*, 2009, **19**, 3042–3048.
- 21 R. Anuwattana, K. J. Balkus Jr, S. Asavapisit and P. Khummongkol, *Microporous Mesoporous Mater.*, 2008, **111**, 260–266.
- 22 Y. K. Hwang, J.-S. Chang, S.-E. Park, D. S. Kim, Y.-U. Kwon, S. H. Jung, J.-S. Hwang and M. S. Park, *Angew. Chem.*, 2005, **117**, 562–566.
- 23 N. C. Maiti, S. Mazumdar and N. Periasamy, *J. Phys. Chem. B*, 1998, **102**, 1528–1538.
- 24 M. Fang, Y. Wang, P. Zhang, S. Li and R. Xu, *J. Lumin.*, 2000, **91**, 67–70.
- 25 P. Zhang, J. Guo, Y. Wang and W. Pang, *Mater. Lett.*, 2002, **53**, 400–405.
- 26 D. Chen, D. Yang, J. Geng, J. Zhu and Z. Jiang, *Appl. Surf. Sci.*, 2008, **255**, 2879–2884.
- 27 D. M. Crizer and S. A. McLuckey, *J. Am. Soc. Mass Spectrom.*, 2009, **20**, 1349–1354.
- 28 Sujandi, S.-E. Park, D.-S. Han, S.-C. Han, M.-J. Jin and T. Ohsuna, *Chem. Commun.*, 2006, 4131–4133.